CORROSION SCIENCE AND TECHNOLOGY, Vol.23, No.6(2024), pp.562~568 pISSN 1598-6462 / eISSN 2288-6524
[Research Paper] DOI: https://doi.org/10.14773/cst.2024.23.6.562

Corrosion Protection of Electrogalvanized Steel Sheet by Chromate-free Coating with Tetravalent Vanadium Ions

Takeshi Matsuda[1,†], Shinichi Furuya[1], Rie Kaneko[1], and Koji Fushimi[2]

[1]*Coated Products Research Department, JFE Steel Corporation, Fukuyama 7218510, Japan*
[2]*Division of Materials Chemistry, Graduate School of Engineering, Hokkaido University, Sapporo 0608628, Japan*
(Received January 29, 2024; Revised April 15, 2024; Accepted April 15, 2024)

The corrosion-protective behavior of electrogalvanized steel sheets (EG) by tetravalent vanadium ions was investigated. The immersion of bare EG in a NaCl solution revealed that the cathodic reactivity to form vanadium (III) oxide on the EG surface decreased when vanadium (IV) oxide sulfate was added to the solution. Characterization of the corrosion products by X-ray photoelectron spectroscopy revealed that vanadium (III) precipitated as V_2O_3 on the EG surface, while ZnO was also included in the corrosion products. It was assumed that vanadium (IV) species was reduced to vanadium (III) simultaneously with the oxidation of zinc, and V_2O_3 precipitates immediately on the EG surface. The corrosion-protective ability of an epoxy coating containing vanadium (IV) species was investigated by a salt spray test. The white rust area of EG coated with vanadium (IV) species was smaller than that without vanadium (IV). Since the reduction reaction of vanadium (IV) species followed by the precipitation of V_2O_3, which has a high corrosion protection ability, indicated a corrosion-protective process similar to that of chromium (VI) ions, vanadium (IV) species was concluded as a candidate inhibitor for chromate-free coatings.

Keywords: *Corrosion protection, Vanadium (IV) ion, Electrogalvanized steel sheet, Epoxy coating*

1. Introduction

Galvanized steel sheets are widely used in automobiles, electrical machinery and building materials because of the anti-corrosion effect on steel sheets. Among these products, electrogalvanized steel sheets (EG) are used in electrical machinery such as home appliances and office automation equipment because of their uniform metallic luster. It is important to protect zinc coatings from corrosion because corrosion products such as zinc oxide degrade the appearance of electrical machinery. A chromate coating consisting of chromium (III) oxide and a small amount of chromium (VI) was applied to prevent corrosion of EG [1-4]. Chromate coatings feature a high barrier property against corrosive species and good adhesion to metal substrates because chromium (III) oxide can be polymerized and bonded to metal substrates [1,5-9]. A self-healing ability is also a characteristic because a polymeric coating composed of chromium (III) oxide is formed in defective or damaged parts of the coating by the reduction reaction of chromium (VI) ions [2,8-10]. Thus, chromate coatings can achieve excellent corrosion protection with a thin coating layer and maintain the metallic appearance of the substrate. However, strict regulations have been applied to the use of certain heavy metals such as Cd, Pb, Hg and Cr(VI) due to their high toxicities, as seen, for example, in the "Restriction of Hazardous Substances (RoHS) Directive" enforced in Europe from 2003 [11]. Thus, alternative coating systems are needed for corrosion protection of EG.

Vanadium (IV) species are known to form a sol-gel coating consisting of a dense oxide and/or hydroxide coating by hydrolysis of the oxovanadate ion VO^{2+}. In particular, when the metal substrate is immersed in an acidic solution of sodium metavanadate $NaVO_3$ [12-17] or ammonium metavanadate NH_3VO_3 [18-20], a sol-gel coating consisting of a complex oxide of vanadium (V) species and vanadium (IV) species is formed by an etching reaction on the metal surface [15,21,22]. When this sol-gel coating is formed on EG, hydrolysis of the vanadium (V) species proceeds while incorporating oxidatively dissolved Zn(II) species into the coating by the etching reaction, and the sol-gel coating is obtained by the dehydration condensation reaction of the product

†Corresponding author: t-matsuda@jfe-steel.co.jp

$V^{V}O(OH)_3(OH_2)_2$. It has been reported that the anodic reaction is remarkably suppressed due to the synergistic effect of the adhesion of the interface between the galvanizing and coating and the barrier property of the polymerized sol-gel coating [15,23]. However, due to the formation of the V(V) decavanadate ion $V_{10}O_{28}^{6-}$, which has a low corrosion protection ability depending on the pH and V(V) concentration of the acidic solution [12,22], practical application of this technology is expected to be challenging. On the other hand, sol-gel coatings composed of V(IV), in which decavanadate ions are not produced, have been studied. It has been reported that sol-gel coatings composed of the vanadium (IV) species are expected to be used as a substitute for chromate coatings because they are likely to ensure the adhesion property, barrier property and self-healing ability with the same coating components [24-27]. In this study, the open circuit potential (OCP) of a bare EG sheet in a NaCl solution containing only the vanadium (IV) species is monitored, and the corrosion products on the EG surface are analysed by X-ray photoelectron spectroscopy (XPS). The corrosion resistance of EG coated with an epoxy resin containing the vanadium (IV) species is also evaluated by a salt spray test (SST).

2. Experimental Methods

2.1 Materials

As the test steel material, 0.6 mm thick EG sheets with a zinc coating thickness of 2.8 μm were obtained from JFE Steel Corporation. Polyvinyl chloride (PVC) tape was purchased from Nitto Denko Corporation. Vanadium (IV) oxide sulfate hydrate ($VOSO_4 \cdot xH_2O$) was purchased from Shinko Chemical Co., Ltd. Epoxy resin (Beckopox™ VEP 2381 W/55WA) and an amine hardener (Beckopox™ EH 623 W/80WA) were supplied by Allnex. Fine Cleaner E6403 was purchased from Nihon Parkerizing Co., Ltd. Deionized water was used for all experiments. All solvents and reagents were used without further purification.

2.2 Immersion test

The EG sheets were cut to a size of 150 mm × 50 mm and defatted with Fine Cleaner E6403 to remove corrosion inhibiting oil and used as specimens. The four ends of the specimens were sealed with PVC tape, and the specimens were immersed in a 5 wt% NaCl solution with or without 1 mM $VOSO_4$ at ambient temperature. After immersion, the specimens were rinsed with water and air-dried. Samples exposed to the solution for a period of time were evaluated visually.

2.3 Characterization

OCP measurement of the specimens was performed by the three-electrode technique using a platinum counter electrode and a silver/silver chloride reference electrode. The EG specimens were immersed in a 5 wt% NaCl solution with or without 1 mM $VOSO_4$, and OCP was measured continuously at ambient temperature. The surfaces of the EG specimens immersed in a 5 wt% NaCl solution with or without 1 mM $VOSO_4$ were analysed with an XPS (ULVAC-PHI Quantera SXM). Al Kα was used as the X-ray source, and binding energy of C 1s (284.8 eV) was used for correction of the electrostatic charge.

2.4 Salt spray test

The EG sheets were cut to a size of 150 mm × 50 mm and degreased with Fine Cleaner E6403 to remove corrosion inhibition oil, and were then used as specimens. 5 wt% of $VOSO_4$ was added to an epoxy resin with a stoichiometric amount of an amine hardener. The total amount of solid in the paint was adjusted by adding water so that a 1 μm thick dry film was achieved. The SST was conducted by spraying the specimen with a 5 wt% NaCl solution and holding the specimen in air with a 95 %RH at 35 ºC in accordance with JIS Z 2371. Visual assessments were performed at periodic intervals.

3. Results and Discussion

3.1 Immersion test of bare EG

The time variation of the OCP of the bare EG immersed in the 5 wt% NaCl solution containing 1 mM $VOSO_4$ was measured. (Fig. 1). For comparison, a 5 wt% NaCl solution without $VOSO_4$ was also used. Regardless of the presence or absence of $VOSO_4$, the OCP immediately after immersion was unstable and rapidly shifted in the less noble direction. Because the bare EG is not covered with a highly corrosion-resistant natural oxide such as an aluminium alloy, the rapid change in potential immediately

after immersion is presumed to be due to activation of the anodic reaction of Zn. OCP was stable in the 5 wt% NaCl solution without $VOSO_4$ from –0.80 to –0.81 V_{SHE}. Since this roughly corresponds to the standard electrode potential of Zn, –0.76 V_{SHE}, the formation of the zinc (II) species by oxidation of Zn is thought to proceed. On the other hand, in the solutions containing $VOSO_4$, the OCP shifted in the noble direction after reaching its lowest potential, and then showed a lower potential than in the solutions without $VOSO_4$ and remained between –0.82 and –0.83 V_{SHE}. These changes in OCP indicate that $VOSO_4$ affects the reaction of bare EG in a NaCl solution.

Fig. 2 shows the surface appearance of a specimen immersed in a NaCl solution for 24 hours. In the NaCl solution without $VOSO_4$, gray dots can be observed in the glossy part of the specimen (Fig. 2b). White products were also continuously deposited on the sample surface in the gray dots. In contrast, the entire surface of the specimen immersed in the NaCl solution containing $VOSO_4$ became dark gray, indicating that some products were deposited on the EG surface in the solution containing $VOSO_4$ (Fig. 2c). The transition of OCP to less noble is thought to be highly relevant to the formation of these deposits.

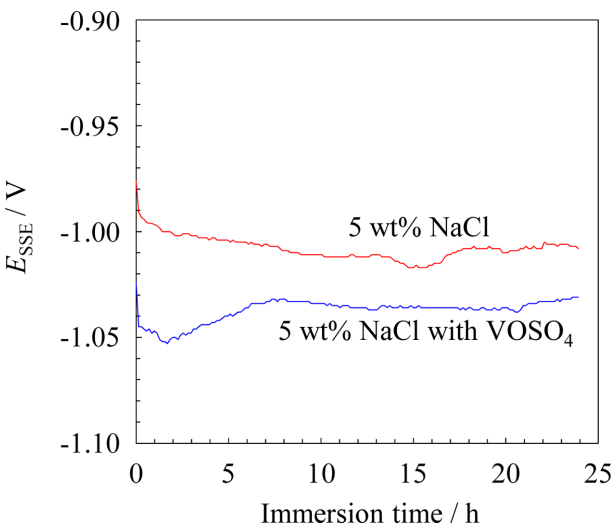

Fig. 1. Time-variation in OCP of EG immersed in 5 wt% NaCl solution with or without $VOSO_4$

3.2 Characterization of corrosion products

The surfaces after immersion in the NaCl solutions containing $VOSO_4$ for 3 and 24 hours were analysed by XPS to determine the chemical state of the products. In the wide-scan spectrum, peaks attributed to Zn, V or O were detected (Fig. 3). Fig. 4a shows the narrow scan spectra of the Zn Auger L3M45M45 line with peak binding energies at 494.6 eV and 497.8 eV, which are nearly identical with those of Zn (494.5 eV) [28] and ZnO (498.0 eV) [28], respectively. The increase in the ratio of ZnO to Zn with immersion time suggests that ZnO is gradually deposited on the EG surface. Fig. 4b shows the narrow scan spectra of $V2p_{3/2}$. The peak binding energy of $VOSO_4$ is 516.7 eV, which is substantially in agreement with the 516.3 eV of $V(IV)O_2$ [28]. In comparison, the peak binding energy of the product deposited on the EG surface is 515.7 eV, which is about 1 eV smaller than that of vanadium (IV) independent of immersion time and is consistent with the peak energy of $V(III)_2O_3$ (515.7 eV) [28], indicating that the product V exists in a trivalent form. On the other hand, the narrow scan spectra (Fig. 4c) of O1s shows a peak binding energy at 530.4 eV regardless

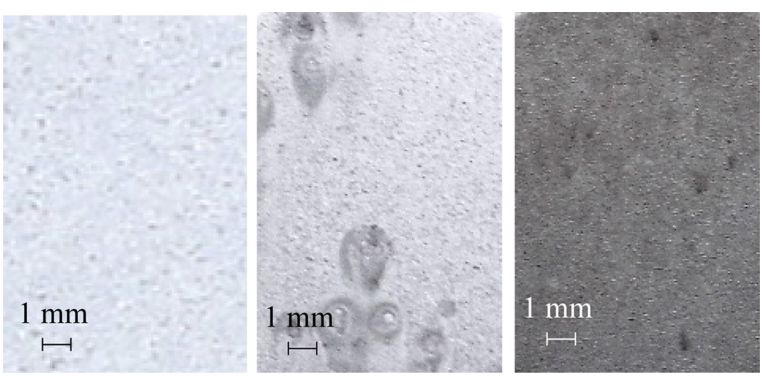

Fig. 2. Photographs of EG surfaces immersed in 5 wt% NaCl solution without $VOSO_4$ for (a) 0 h and (b) 24 h or (c) with $VOSO_4$ for 24 h

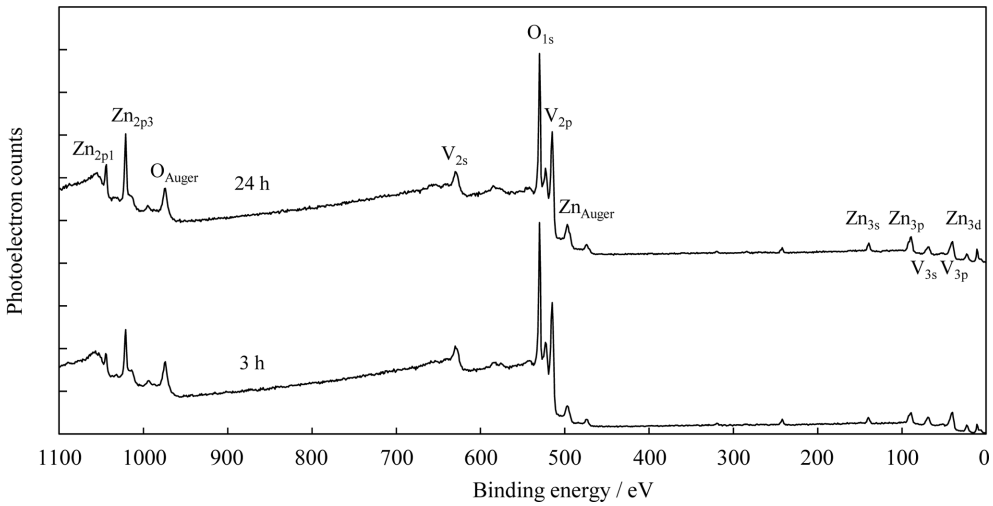

Fig. 3. XPS spectrum of EG surface immersed in 5 wt% NaCl solution with $VOSO_4$

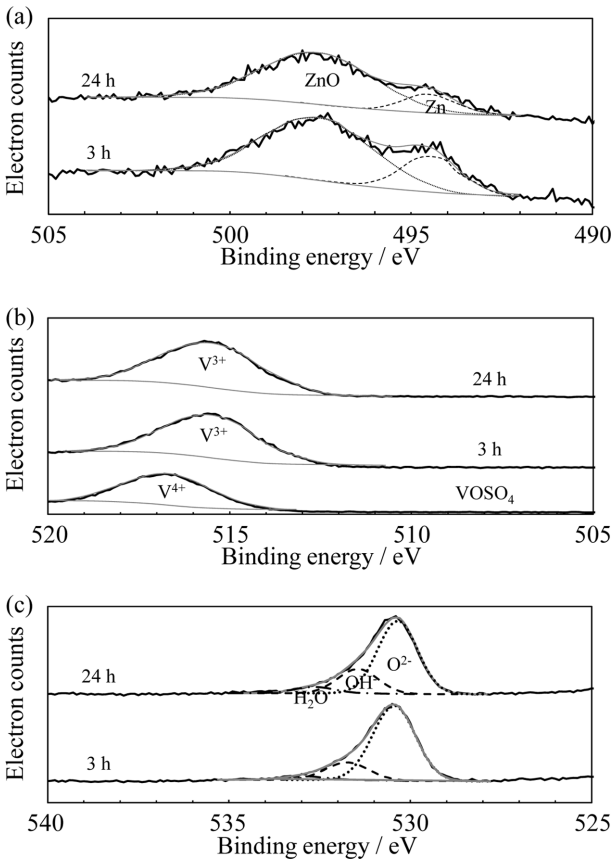

Fig. 4. High resolution XPS spectrum of (a) Z_{Auger}, (b) $V2p_{3/2}$ and (c) O1s obtained for $VOSO_4$ and EG immersed in 5 wt% NaCl solution with $VOSO_4$

of immersion time. The results of deconvolution using the peaks of O^{2-} (530.5 eV) [28], OH^- (531.8 eV) [28] and H_2O (533.0 eV) [28] are shown in Table 1. It is found that the vanadium (IV) species are reduced to vanadium

Table 1. Deconvolution ratio of Zn_{Auger} and O1s spectrum with immersion time

	Zn_{Auger}		O1s		
	ZnO	Zn	O^{2-}	OH^-	H_2O
3 hours	77	23	78	18	4.0
24 hours	86	14	70	24	6.0

(III) species consisting mainly of V_2O_3 and vanadium (III) hydroxides such as VO(OH) and $V(OH)_3$, or a small amount of hydrate, which are deposited on the EG surface.

Here, the potential-pH diagram of the V-H_2O system generated by OLI Studio (Fig. 5) is used to examine the formation process of V_2O_3 on the EG surface. The maximum consumption of the vanadium (IV) species in the NaCl solution in the 24-hour immersion test was about 0.05 mM, which is two orders smaller than the original concentration. Therefore, when creating the diagram, the concentration of V is assumed to be 1 mM. Reductive precipitation of the vanadium (IV) species dissolved in the NaCl solution requires oxidation of the dissolved species or the EG surface. The redox potential of Zn(II)/Zn is –0.76 V_{SHE}, while that of V(IV)/V(III) is 0.34 V_{SHE} [29]. There is no doubt that zinc acts as a reducing agent because the NaCl solutions contain no other substances that act as reducing agents. Therefore, when zinc is oxidized and eluted as the zinc (II) species, the vanadium (IV) species near the EG surface is reduced to the vanadium (III) species. In a neutral NaCl solution, the vanadium (III) species are considered to precipitate

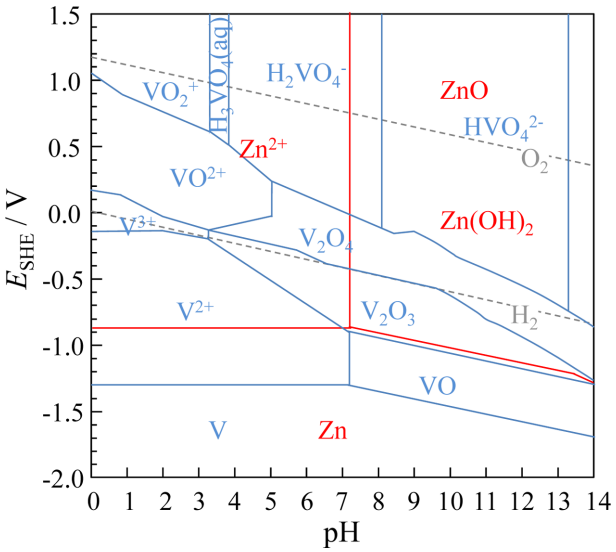

Fig. 5. Pourbaix diagram of V and Zn. The concentration of the elements is10^{-3} M

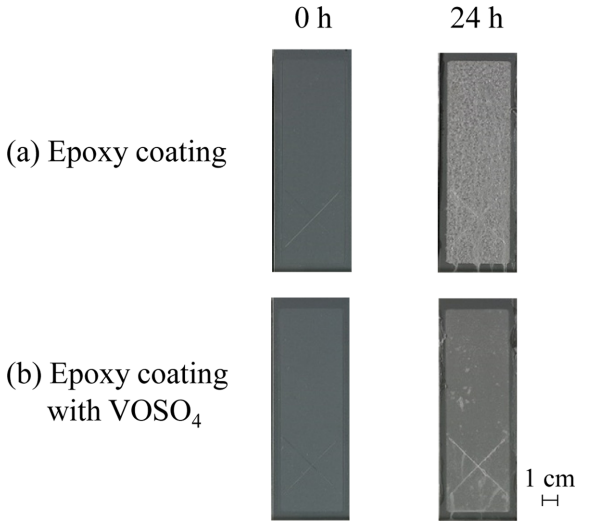

Fig. 6. Photographs of specimens coated with (a) epoxy resin and (b) epoxy resin containing 5 wt% of $VOSO_4$ after SST for 24 hours

immediately as V_2O_3 in an environment which is more than weakly acidic, and the EG surface is then covered with V_2O_3. Since the solubility products of $V(OH)_3$ and $Zn(OH)_2$ are 4×10^{-35} and 3×10^{-17} [30], respectively, V_2O_3 is thought to precipitate prior to ZnO, but a small amount of ZnO is also likely to be present. Considering the results of the OCP immediately after immersion of the bare EG in the 5 wt% NaCl solution containing $VOSO_4$ (Fig. 1), the rapid shift in a less noble direction is related to the acceleration of zinc oxidation by the vanadium (IV) species. After reaching the lowest potential, the OCP in the solution containing $VOSO_4$ shifts in the noble direction, indicating that oxidation of zinc may be suppressed by precipitation of V_2O_3 on the EG surface.

3.3 SST

Fig. 6 shows photographs of the EGs coated with an epoxy coating with or without $VOSO_4$ having an artificial cross-cut scratch before and after the SST for 24 hours. White rust occurred over the entire surface of the specimen coated with the epoxy resin, while slightly white rust was observed on the specimen coated with epoxy resin containing $VOSO_4$. Since white rust is derived from zinc oxide, the EG coated with an epoxy coating without $VOSO_4$ is severely corroded. This suggests that corrosion resistance of epoxy resin coating is not sufficient, and both the anodic reaction by zinc dissolution and the cathodic reaction by oxygen reduction actively occur. In contrast, the occurrence of white rust was suppressed on the EG coated with an epoxy coating containing $VOSO_4$. It is considered that corrosion resistance was improved by suppression of the cathodic reaction due to the self-healing reaction of forming an oxide film of Zn and vanadium (III) species when the vanadium (IV) species in the epoxy coating is dissolved in a corrosion environment.

4. Conclusions

The corrosion protection behavior of EG by vanadium (IV) ions was investigated. Addition of $VOSO_4$ at a concentration of 1 mM to a 5 wt% NaCl solution shifted the OCP of the bare EG toward the less noble direction. In the early stage of immersion, zinc was oxidized simultaneously with the reduction of the vanadium (IV) species in the NaCl solution to the vanadium (III) species, and the vanadium (III) species precipitated immediately as V_2O_3 in the NaCl solution. As the corrosion resistance of the EG coated with the epoxy resin containing V_2O_3 was improved, it was concluded that the vanadium (IV) species is a candidate inhibitor for chromate-free coatings.

References

1. N. M. Martyak, J. E. McCaskie and L. Harrison, Corrosion behavior of zinc chromate coatings, *Metal Finishing*, **94**, 65 (1996). Doi: https://doi.org/10.1016/S0026-0576(96)93872-6
2. X. Zhang, S. Böhm, A. J. Bosh, E. P. M. van Westing, J. H. W. de Wit, Influence of drying temperature on the corrosion performance of chromate coatings on galvanized steel, *Materials and Corrosion*, **55**, 501 (2004). Doi: https://doi.org/10.1002/maco.200303769
3. F. W. Eppensteiner, M. R. Jenkins, Chromate conversion coatings, *Metal Finishing*, **93**, 460 (1995). Doi: https://doi.org/10.1016/0026-0576(95)93395-I
4. F. W. Eppensteiner, M. R. Jennkind, Chromate conversion coatings, *Metal Finishing*, **105**, 413 (2007). Doi: https://doi.org/10.1016/S0026-0576(07)80360-6
5. L. F. G. Williams, The initiation of corrosion of chromated zinc electroplate on steel, *Corrosion Science*, **13**, 865 (1973). Doi: https://doi.org/10.1016/S0010-938X(73)80068-X
6. A. Suda, T. Ogino, T. Miyawaki and S. Maeda, Structural Changes in Dry-in-place Chromate Film at Various Drying Temperature, *Journal of The Surface Finishing Society of Japan*, **44**, 841 (1993). Doi: https://doi.org/10.4139/sfj.44.841
7. A. Suda, T. Shinohara, S. Tsujikawa, T. Ogino and S. Tanaka, *Proc. 2nd. Int. Conf. on zinc and zinc alloy coated steel sheet*, p. 250, Chicago, USA (1992).
8. X. Zhang, W. G. Sloof, A. Hovestad, E. P. M. van Westing, H. Terryn, J. H. W. de Wit, Characterization of chromate conversion coatings on zinc using XPS and SKPFM, *Surface* and *Coatings Technology*, **197**, 168 (2005). Doi: https://doi.org/10.1016/j.surfcoat.2004.08.196
9. X. Zhang, C. van den Bos, W. G. Sloof, A. Hovestad, H. Terryn, J. H. W. de Wit, Comparison of the morphology and corrosion performance of Cr(VI)- and Cr(III)-based conversion coatings on zinc, *Surface and Coatings Technology*, **199**, 92 (2005). Doi: https://doi.org/10.1016/j.surfcoat.2004.12.002
10. R. J. Sunderland, *Proc. 6th Int. Vac. Congr.*, p. 347, Kyoto, Japan (1974).
11. Official Journal of European Union, L37 (2003). https://op.europa.eu/en/publication-detail/-/publication/9b9ccfd5-0707-4c6a-bec7-0e5a49931f41
12. K. D. Ralston, S. Chrisanti, T. L. Young, R. G. Buchheit, Corrosion Inhibition of Aluminum Alloy 2024-T3 by Aqueous Vanadium Species, *Journal of The Electrochemical Society*, **155**, C350 (2008). Doi: https://doi.org/10.1149/1.2907772
13. L. Niu, S. H. Chang, X. Tong, G. Li, Z. Shi, Analysis of characteristics of vanadate conversion coating on the surface of magnesium alloy, *Journal of Alloys and Compounds*, **617**, 214 (2014). Doi: https://doi.org/10.1016/j.jallcom.2014.08.044
14. K. H. Yang, M. D. Ger, W. H. Hwu, Y. Sung, Y. C. Liu, Study of vanadium-based chemical conversion coating on the corrosion resistance of magnesium alloy, *Materials Chemistry and Physics*, **101**, 480 (2007). Doi: https://doi.org/10.1016/j.matchemphys.2006.08.007
15. Z. Zou, N. Li, D. Li, H. Liu, S. Mu, A vanadium-based conversion coating as chromate replacement for electrogalvanized steel substrates, *Journal of Alloys and Compounds*, **509**, 503 (2011). Doi: https://doi.org/10.1016/j.jallcom.2010.09.080
16. P. Wang, X. Dong, D. W. Schaefer, Structure and water-barrier properties of vanadate-based corrosion inhibitor films, *Corrosion Science*, **52**, 943 (2010). Doi: https://doi.org/10.1016/j.corsci.2009.11.017
17. X. Zhong, X. Wu, Y. Jia, Y. Liu, Self-repairing vanadium–zirconium composite conversion coating for aluminum alloys, *Applied Surface Science*, **280**, 489 (2013). Doi: https://doi.org/10.1016/j.apsusc.2013.05.015
18. Y. Ma, N. Li, D. Li, M. Zhang, X. Huang, Characteristics and corrosion studies of vanadate conversion coating formed on Mg–14 wt%Li–1 wt%Al–0.1 wt%Ce alloy, *Applied Surface Science*, **261**, 59 (2012). Doi: https://doi.org/10.1016/j.apsusc.2012.07.069
19. X. Chen, G. Li, J. Lian, Q. Jiang, An organic chromium-free conversion coating on AZ91D magnesium alloy, *Applied Surface Science*, **255**, 2322 (2008). Doi: https://doi.org/10.1016/j.apsusc.2008.07.092
20. X. Chen, G. Li, J. Lian, Q. Jiang, Study of the formation and growth of tannic acid based conversion coating on AZ91D magnesium alloy, *Surface and Coatings Technology*, **204**, 736 (2009). Doi: https://doi.org/10.1016/j.surfcoat.2009.09.022
21. M. Iannuzzi, G. S. Frankel, Mechanisms of corrosion inhibition of AA2024-T3 by vanadates, *Corrosion Science*, **49**, 2371 (2007). Doi: https://doi.org/10.1016/j.corsci.2006.10.027
22. M. Iannuzzi, J. Kovac, G. S. Frankel, A study of the mechanisms of corrosion inhibition of AA2024-T3 by vanadates using the split cell technique, *Electrochimica Acta*, **52**, 4032 (2007). Doi: https://doi.org/10.1016/j.electacta.2006.11.019

23. N. E. Akulich, I. M. Zharskii, N. P. Ivanova, A Study of Conversion Coatings on Vanadium/Galvanic Zinc, *Protection of Metals and Physical Chemistry of Surfaces* , **53**, 503 (2017). Doi: https://doi.org/10.1134/S2070205117020034
24. Z. Gao, D. Zhang, S. Jiang, Q. Zhang, X. Li, XPS investigations on the corrosion mechanism of V(IV) conversion coatings on hot-dip galvanized steel, *Corrosion Science*, **139**, 163 (2018). Doi: https://doi.org/10.1016/j.corsci.2018.04.030
25. Z. Gao, D. Zhang, X. Qiu, S. Jiang, Y. Wu, Q. Zhang, X. Li, The mechanisms of corrosion inhibition of hot-dip galvanized steel by vanadyl oxalate: A galvanic corrosion investigation supported by XPS, *Corrosion Science*, **142**, 153 (2018). Doi: https://doi.org/10.1016/j.corsci.2018.07.024
26. Z. Gao, D. Zhang, L. Hou, X. Li, Y. Wei, Understanding of the corrosion protection by V(IV) conversion coatings from a sol-gel perspective, *Corrosion Science*, **161**, 108196 (2019). Doi: https://doi.org/10.1016/j.corsci.2019.108196
27. Zhongli Zou, Ning Li, Deyu Li, Haiping Liu, Songlin Mu, A vanadium-based conversion coating as chromate replacement for electrogalvanized steel substrates, *Journal of Alloys and Compounds*, **509**, 503 (2011). Doi: https://doi.org/10.1016/j.jallcom.2010.09.080
28. C. D. Wanger, W. M. Riggs, L. E. Davis, J. F. Moulder, G. E.Muilenberg, *Handbook of X-ray Photoelectron Spectroscopy*, Perkin-Elmer Corp., Physical Electronics Division, Eden Prairie, Minnesota, USA (1979).
29. X. Li, H. Zhang, Z. Mai, H. Zhang I. Vankelecom, Ion exchange membranes for vanadium redox flow battery (VRB) applications, *Energy & Environmental Science*, **4**, 1147 (2011). Doi: https://doi.org/10.1039/C0EE00770F
30. Engineering ToolBox, https://www.engineeringtoolbox.com/solubility-product-equilibrium-constant-ionic-solution-salt-Ksp-d_1952.html (2001).